Crystal structure of JNK3: a kinase implicated in neuronal apoptosis

Xiaoling Xie*, Yong Gu, Ted Fox, Joyce T Coll, Mark A Fleming, William Markland, Paul R Caron, Keith P Wilson and Michael S-S Su*

Background: The c-Jun N-terminal kinases (JNKs) are members of the mitogen-activated protein (MAP) kinase family, and regulate signal transduction in response to environmental stress. Activation and nuclear localization of JNK3, a neuronal-specific isoform of JNK, has been associated with hypoxic and ischemic damage of CA1 neurons in the hippocampus. Knockout mice lacking JNK3 showed reduced apoptosis of hippocampal neurons and reduced seizure induced by kainic acid, a glutamate-receptor agonist. Thus, JNK3 may be important in the pathology of neurological disorders and is of significant medical interest.

Results: We report here the structure of unphosphorylated JNK3 in complex with adenylyl imidodiphosphate, an ATP analog. JNK3 has a typical kinase fold, with the ATP-binding site situated within a cleft between the N- and C-terminal domains. In contrast to other known MAP kinase structures, the ATP-binding site of JNK3 is well ordered; the glycine-rich nucleotide-binding sequence forms a β-strand–turn–β-strand structure over the nucleotide. Unphosphorylated JNK3 assumes an open conformation, in which the N- and C-terminal domains are twisted apart relative to their positions in cAMP-dependent protein kinase. The rotation leads to the misalignment of some of the catalytic residues. The phosphorylation lip of JNK3 partially blocks the substrate-binding site.

Conclusions: This is the first JNK structure to be determined, providing a unique opportunity to compare structures from the three MAP kinase subfamilies. The structure reveals atomic-level details of the shape of JNK3 and the interactions between the kinase and the nucleotide. The misalignment of catalytic residues and occlusion of the active site by the phosphorylation lip may account for the low activity of unphosphorylated JNK3. The structure provides a framework for understanding the substrate specificity of different JNK isoforms, and should aid the design of selective JNK3 inhibitors.

Address: Vertex Pharmaceuticals Incorporated, 130 Waverly Street, Cambridge, MA 02139-4211, USA.

*Corresponding authors.
E-mail: su@vpharm.com
          xie@vpharm.com

Introduction

Mammalian cells respond to extracellular stimuli by activating members of the mitogen-activated protein (MAP) kinase family, which include the extracellular signal regulated kinases (ERKs), the p38 MAP kinases and the c-Jun N-terminal kinases (JNKs). MAP kinases are serine/threonine kinases that are activated by dual phosphorylation of threonine and tyrosine residues of the Thr-X-Tyr segment in a loop located adjacent to the active site [1,2]. Phosphorylation of each MAP kinase is carried out by specific kinases upstream of MAP kinase. Activated MAP kinases then phosphorylate various substrates, including transcription factors, which in turn regulate the expression of specific sets of genes and thus mediate a specific response to the stimulus.

Members of the JNK family of kinases are activated by proinflammatory cytokines tumor necrosis factor-α and interleukin-1β as well as environmental stress, such as anisomycin, UV irradiation, hypoxia and osmotic shock [2]. Three distinct genes encoding JNKs, Jnk1, Jnk2 and Jnk3, have been identified and at least ten different splicing isoforms exist in mammalian cells [3]. The downstream substrates of JNKs include the transcription factors c-Jun, ATF-2, Elk1, NFAT, p53 and a cell death domain protein [4–9]. Each JNK isoform binds to these substrates with different affinities, suggesting a regulation of signaling pathways by substrate specificity of different JNKs *in vivo* [3].

JNK1 and JNK2 are widely expressed in a variety of tissues. In contrast, JNK3 is selectively expressed in the brain and to a lesser extent in the heart and testis [3,10,11]. In the adult human brain, JNK3 expression is localized to a subpopulation of pyramidal neurons in the CA1, CA4 and subiculum regions of the hippocampus and layers 3 and 5 of the neocortex [10]. The CA1 neurons in brain biopsies of patients diagnosed with acute hypoxia showed strong nuclear JNK3 immunoreactivity. In contrast, control

samples taken from patients with nonneuronal diseases revealed only diffused cytoplasmic JNK3 staining in the hippocampal neurons [9]. Furthermore, disruption of the JNK3 gene caused resistance of mice to the excitotoxic glutamate receptor agonist kainic acid, including the effects on seizure activity, AP-1 transcriptional activity and apoptosis of hippocampal neurons, indicating that the JNK3 signaling pathway is a critical component in the pathogenesis of glutamate neurotoxicity [12]. Thus, selective modulation of JNK3 activity could potentially provide therapeutic intervention for neurodegenerative diseases such as stroke and epilepsy.

To help understand the regulation of JNK3, and other members of the JNK subfamily of protein kinases, we have solved the crystal structure of unphosphorylated JNK3α1 in complex with adenylyl imidodiphosphate (AMP-PNP) and magnesium at 2.3 Å resolution. This is the first JNK structure to be solved and, together with p38 and ERK2, provides a unique opportunity to compare structures across the MAP kinase family.

Results and discussion

### Crystallization of JNK3 in complex with MgAMP-PNP

Human JNK3α1 has an extended N terminus when compared to JNK1, JNK2 and other MAP kinases (Figure 1)

[3]. For the purpose of crystallographic studies a truncated form of JNK3, without the first 39 residues, was expressed. Crystallization trials of this form of the enzyme yielded small crystals that diffracted to 8 Å. Because residues at the C terminus of ERK2 and p38 are disordered [13,14], we reasoned that the C-terminal residues of JNK3 might also be flexible and interfere with the formation of a well ordered crystal lattice. We therefore searched for an active shortened form of JNK3 with C-terminal truncation of the protein. JNK3 protein lacking the N-terminal 39 and C-terminal 20 residues was found to display similar kinase activity to the JNK3 protein without the C-terminal truncation when activated by MAP kinase kinase 7 (MKK7) [15] *in vitro* (see Materials and methods section). This form of the protein could be used to grow large, well-ordered crystals that diffract to at least 2.3 Å resolution. The structure of JNK3 was solved using this truncated enzyme (residues Ser40–Glu402).

Overall structure

The MAP kinase homologous region of JNK3 (residues Phe48–Glu397) is 45% identical in amino acid sequence to ERK2 and 51% identical to p38, the structures of which have been reported [13,14] (Figure 1). As expected, the overall architecture of JNK3 is highly similar to that of ERK2 and p38. The N-terminal domain (residues 45–149

Figure 1
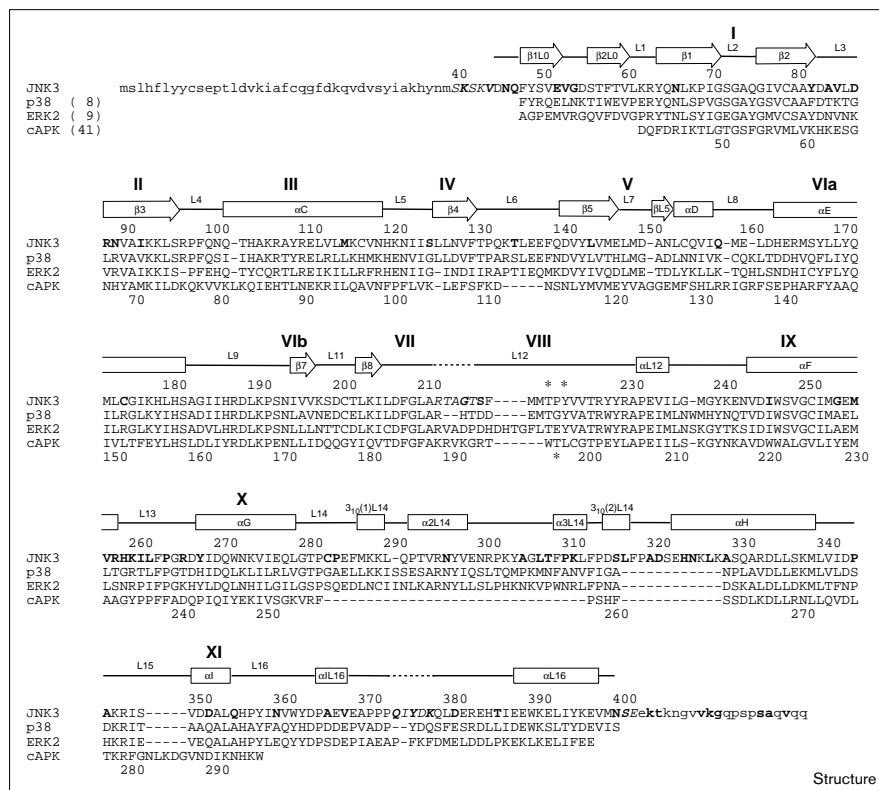
Structure-based sequence alignment of JNK3, p38, ERK2 and cAPK. The amino acid sequences of human JNK3 [3], human p38 kinase [34], human ERK2 [35] and murine cAPK [36] are aligned based on structural similarity. The divergent N- and C-terminal regions of p38, ERK2 and cAPK are not shown. The N- and C-terminal residues that were not included in the truncated JNK3 (residues Ser40–Glu402) used for crystallographic studies are denoted by lowercase letters. Residues omitted from the model are italicized. The subdomains are labeled by Roman numerals according to reference [37]. The secondary structure elements for JNK3 are indicated above the sequences (nomenclature as for Figure 2a), with open boxes designating α and 3_{10} helices and open arrows designating β strands. Disordered regions are indicated with dashed lines. Both the JNK3 and cAPK sequence numbering are shown, above and below the alignment, respectively. Phosphorylation sites in the phosphorylation lip are denoted by an asterisk. JNK3 residues that differ from JNK1 and JNK2 [3,38,39] are highlighted in bold.

Figure 2
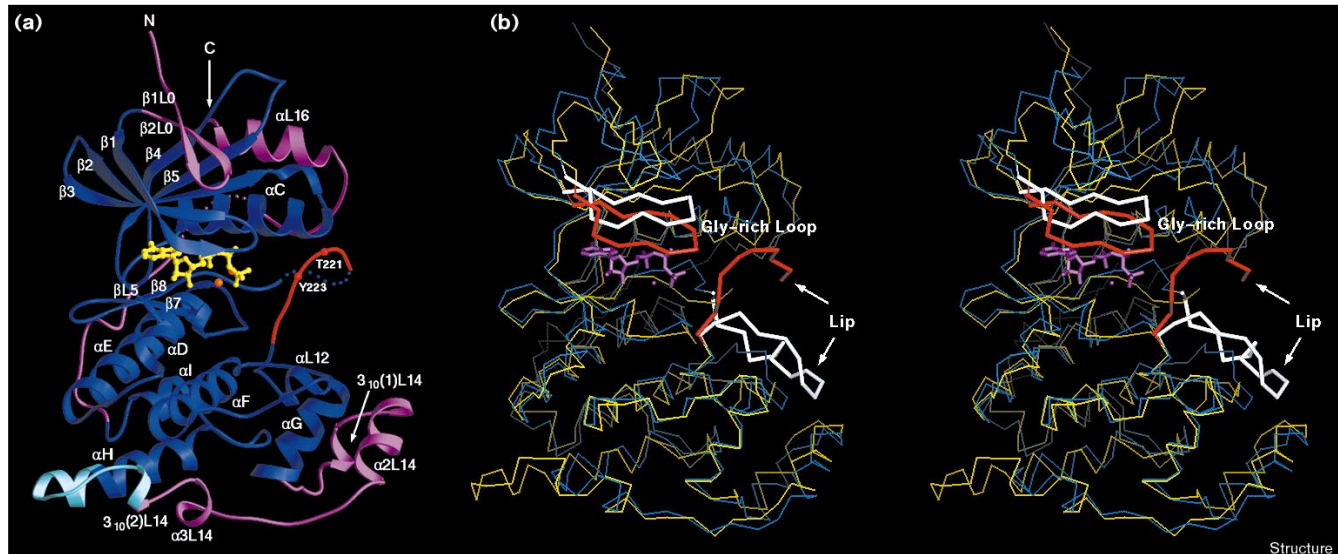
The overall fold of JNK3 and comparison to ERK2. **(a)** Ribbon representation of the overall fold of JNK3 complexed with MgAMP-PNP. Blue indicates secondary structure elements and loops that are conserved among protein kinases; magenta indicates extensions and insertions characteristic for MAP kinases. The JNK insertion (residues Leu317–Lys328) and the phosphorylation lip (residues Ser217–Thr226) are colored in cyan and red, respectively. The bound AMP-PNP (yellow) and two Mg^{2+} ions (orange) are shown in ball-and-stick representation. The Cα positions of the regulatory phosphorylation sites, Thr221 and Tyr223, are shown and labeled. Secondary structure elements are labeled according to [13]. Electron density is not visible for two disordered regions within the core of JNK3 as shown by the dotted lines. One of these disordered regions is Arg212–Thr216 in the C-terminal domain (the corresponding residues in ERK2 form β strand β9 that precedes the phosphorylation lip). The second disordered region includes residues Gln374–Lys378. The structure of phosphorylated ERK2 showed that this portion of L16 is rearranged into a 3_{10} helix upon phosphorylation [19]. (This diagram was constructed using the program RIBBONS [40].) **(b)** Stereoview superposition of JNK3–MgAMP-PNP and ERK2 (entry code 1ERK in the Protein Data Bank [13]). Cα representations of the structures of JNK3 (yellow and red) and ERK2 (blue and white) are shown after superposition of their C-terminal domains. Segments with the largest structural divergence are the glycine-rich loop (residues Gly71–Val78 in JNK3) and the phosphorylation lip (labeled lip; residues Ser217–Thr226 in JNK3), which are highlighted as thick bonds. Superposition of the C-terminal domain of ERK2 onto JNK3 reveals a 2.5 Å shift in the Cα position of Thr226 relative to Thr188 in ERK2. The conformation of Thr226 is also different when compared to Thr188 in ERK2. In JNK3, a pair of water molecules are hydrogen bonded to the mainchain carbonyl and amide groups of Thr226, and mediate interactions with the sidechain of Lys199. As a result, Thr226 adopts different ϕ, ψ angles (Thr226 of JNK3, $\phi = -88°$ and $\psi = 114°$; Thr188 of ERK2, $\phi = -46°$ and $\psi = 130°$), which redirects the path of the phosphorylation lip. Most of the JNK3 residues in the phosphorylation lip (residues Ser217–Thr226) are well ordered, with B factors of the sidechains of Phe209, Leu210, Phe218 and Met220 refined to below 25 Å². In addition, the N-terminal portion of the lip (Ser217–Met220) makes contacts with the N-terminal portion of the αC helix, which in turn contacts the glycine-rich flap covering the nucleotide; the C-terminal portion of the lip (Val225 and Thr226) interacts with part of L9. The residues Thr221–Val224 are solvent exposed. Another significant difference between JNK3 and ERK2 is the position of the glycine-rich loop: the loop in JNK3 is moved towards the triphosphate chain of AMP-PNP, whereas it is partially disordered in ERK2. The glycine-rich loop has conformational flexibility – its rigid conformation is promoted by nucleotide binding.

and 379–400) of JNK3 contains mostly β strands, whereas the C-terminal domain (residues 150–211 and 217–374) is predominantly α helical. A deep cleft between the two domains comprises the ATP-binding site, where the glycine-rich sequence (Gly71-Ser-Gly-Ala-Gln-Gly-Ile-Val78) of JNK3 forms a well-defined β-strand–turn–β-strand structure over the nucleotide. The insertion in the C-terminal domain that is characteristic for MAP kinases is 12 residues longer in JNK3 (residues 283–328) than in ERK2 and p38, resulting in the N-terminal extension of helix αH and an extra 3_{10} helix (Figure 2a). We refer to this 12-residue insertion as 'the JNK insertion' as it is present in all c-Jun N-terminal kinases [3].

The relative orientation of the N- and C-terminal domains is different among the structures of JNK3, ERK2 and p38 (Figure 2b). A superposition of the C-terminal domains of ERK2 and p38 onto the C-terminal domain of JNK3 revealed rotations of the N-terminal domains of ERK2 and p38 by about 2.5° and 4°, respectively. Despite this rotation, the structures of the individual domains of JNK3, ERK2 and p38 are similar. Independent superposition of the N- and C-terminal domains of ERK2 onto JNK3, excluding the phosphorylation lip region, the glycine-rich sequence, the JNK insertion and the protein termini, yielded protein backbone root mean square (rms) deviations of 1.15 Å for the N-terminal domain (residues

Figure 3
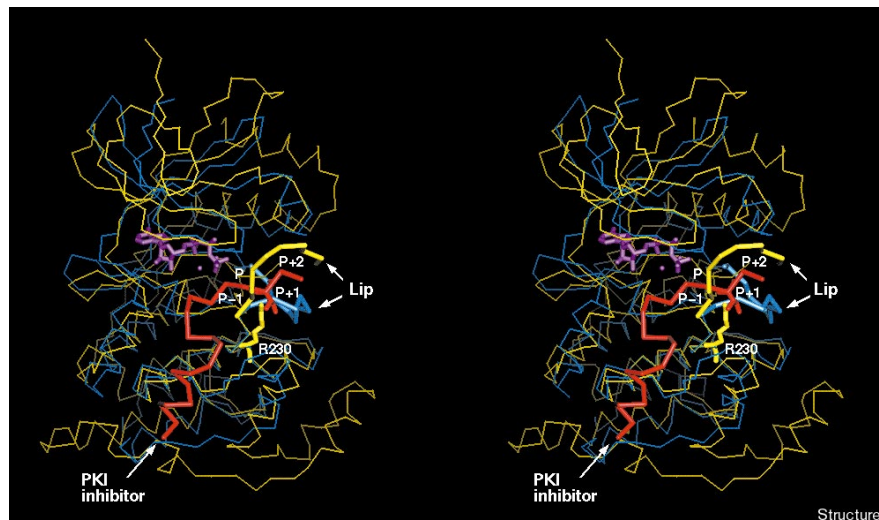
Stereoview superposition of JNK3 and cAPK (entry code 1APK in the Protein Data Bank [16]). Cα representations of JNK3 (yellow) and the cAPK ternary complex (blue and red) are shown after superposition of their C-terminal domains. The phosphorylation lip in JNK3 and cAPK together with the PKI inhibitor (red) are shown as thick bonds. The figure illustrates the difference in the conformation of the lip between the two enzymes, and shows the lip of JNK3 occupying part of the peptide-binding channel. In the cAPK ternary complex, MnAMP-PNP is omitted from the drawing and only the kinase catalytic core portion (residues Asp41–Trp296) of cAPK is shown. P refers to the putative phosphorylation residue of a peptide substrate.

56–149 and 382–400 in JNK3) and 1.58 Å for the C-terminal domain (residues 150–208, 226–315 and 329–369 in JNK3). A similar comparison of JNK3 and p38 showed protein backbone rms deviations of 1.23 Å for the N-terminal domain and 1.60 Å for the C-terminal domain.

The phosphorylation lip
The region spanning residues Ser217–Thr226 contains the JNK3 regulatory phosphorylation sites, Thr221 and Tyr223, and is referred to as the 'phosphorylation lip' or 'activation loop' (Figure 2a). The residue between the two phosphorylation sites in the Thr-X-Tyr tripeptide sequence of JNK3 is proline, whereas this residue is glutamate in ERK2 and glycine in p38. The phosphorylation lip is four residues shorter in JNK3 than in ERK2, and two residues longer than in p38. These differences result in the changes in the position and conformation of the activation residues, and in the path of the phosphorylation lip in the three kinases.

The phosphorylation residues in JNK3 have a different position and conformation when compared to the corresponding amino acids in ERK2 and p38. Thr221 and Tyr223 are 16 Å and 12 Å away from the location of the corresponding residues in ERK2 and p38, respectively. Despite the different locations, the regulatory threonine residues in all three enzymes are solvent exposed. The local environments of the tyrosine residues are different, however. The sidechain of Tyr223 in JNK3 is exposed to solvent and is disordered. The corresponding tyrosine residue in p38 is also solvent accessible, but is well ordered and interacts with the hydroxyl group of Thr221 through a water molecule [14]. In contrast, the sidechain of Tyr185 in unphosphorylated ERK2 is buried, forms a hydrogen bond with the sidechain of Arg146, and makes

van der Waals contacts with nearby hydrophobic amino acid residues [13]. The conformation of Tyr185 in the unphosphorylated ERK2 structure suggests that the phosphorylation lip must be refolded before Tyr185 can become a substrate for the ERK2 upstream activating kinases. A similar movement may not be needed to phosphorylate Thr221 and Tyr223 in JNK3, as these residues are already accessible to solvent in the unphosphorylated form.
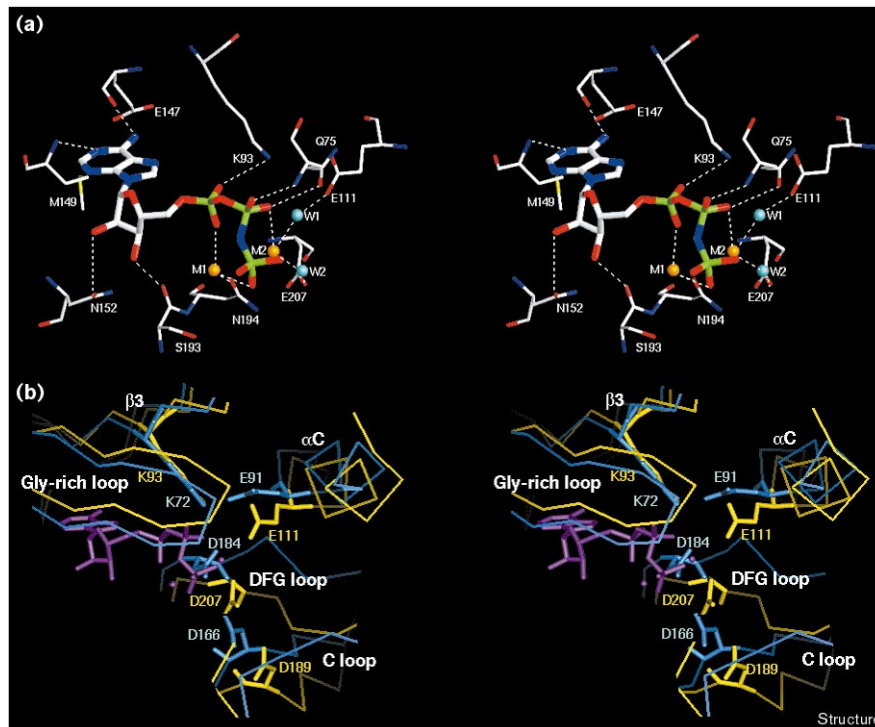
The peptide substrate binding channel
The structure of the ternary complex formed between cAMP-dependent protein kinase (cAPK), the inhibitor peptide PKI(5–24) and MnAMP-PNP, is believed to represent the bioactive conformation for protein kinases [16–18]. The cAPK complex shows that the peptide-binding channel lies mainly in the C-terminal domain, and that the P+1 binding site is formed by a loop (residues Leu198–Leu205 in cAPK) contiguous with the phosphorylation lip and connecting to αL12 (Figure 3). The C-terminal domain of JNK3 superimposes well with that of cAPK. Thus the residues that are likely to be important for JNK3 peptide substrate binding may be mapped by its homology to cAPK (Figure 1).

The protein backbone of residues Arg227–Arg230 in JNK3 has a conformation similar to the corresponding residues in cAPK (residues Pro202–Leu205), but the sidechain of Arg230 fills the P+1 site in an unfavorable conformation for binding substrate (Figure 3). In addition, some of the residues in the JNK3 phosphorylation lip (residues Tyr223–Thr226 in JNK3 corresponding to residues Leu198–Thr201 in cAPK) take a path distinct from that of cAPK and occupy the positions of P–1 to P+2 sites of the peptide substrate (Figure 3).

Figure 4

The active site of JNK3. **(a)** Stereoview of the active site of JNK3. A molecule of AMP-PNP and two Mg^{2+} ions are shown together with their surrounding JNK3 residues. The AMP-PNP molecule is shown as thick bonds and the protein residues as thin bonds. Two Mg^{2+} ions (colored orange and labeled M1 and M2) and two water molecules (colored cyan and labeled W1 and W2) are shown as spheres. Hydrogen bonds are indicated by dashed lines. **(b)** Detailed comparison of the active site of JNK3 with that of cAPK. The figure shows Cα representations of the ATP-binding sites of JNK3 (yellow) and cAPK (blue) with the sidechains of selected residues included. The atoms of AMP-PNP in the JNK3 binary complex and cAPK ternary complex have been superimposed; AMP-PNP is shown in purple. The N-terminal domains of the two enzymes are well aligned, but the difference in domain orientation results in the misalignment of the catalytic residues clustered in the C loop (residues Arg188–Asn194 in JNK3) and DFG loop (residues Asp207–Ala211 in JNK3), such as Asp189 and Asp207, with those in the N-terminal domain, such as Lys93.

Phosphorylation-related conformational changes in the phosphorylation lip as well as the peptide substrate binding channel have been observed in the crystal structures of unphosphorylated and phosphorylated ERK2 [13,19]. Comparison of the JNK3 structure with the structure of phosphorylated ERK2 suggests how phosphorylation at Thr221 and Tyr223 might play a role in the activation of JNK kinases. In the structure of phosphorylated ERK2, phosphothreonine 183 interacts with three arginine residues — Arg68 in αC, Arg146 in the catalytic loop (C loop) and Arg170 from the phosphorylation lip — whereas phosphotyrosine 185 is ligated by Arg189 and Arg192 [19]. If Thr221 and Tyr223 are ligated similarly in the phosphorylated form of JNK3, they would have to move by approximately 15 Å, and a large conformational change of the phosphorylation lip would be required. As a consequence, the restructuring of the phosphorylation lip could help to unblock the peptide substrate binding channel.

The active site

Crystallization of JNK3 with AMP-PNP and Mg^{2+} has yielded structural data for the nucleotide-bound form of JNK3. AMP-PNP is bound in a deep cleft between the two domains of JNK3 (Figure 2a). The binding of the nucleotide analog is similar to that found in the ternary complex formed by cAPK, MnAMP-PNP and the inhibitor peptide PKI(5–24) [16] (Figure 4a). These findings differ from previous crystal soaking experiments with

ERK2 [13], and permit a more detailed description of the interactions between JNK3 and the nucleotide.

Protein kinases contain a nucleotide binding sequence Gly-X-Gly-X-X-Gly-X-X that is referred to as 'the glycine-rich phosphate anchor loop' due to its sequence and role in nucleotide binding [20]. The glycine-rich loop is well defined in JNK3 and superimposes well with that of cAPK, with an rms deviation of 0.54 Å for the protein mainchain atoms from Ile70 to Ser79. The glycine-rich sequence in JNK3 (Gly71-Ser–Gly-Ala-Gln-Gly-Ile-Val78) forms a flap over the nucleotide, covering it almost completely. In contrast, the glycine-rich loops of the apo forms of ERK2 and p38 are partially disordered.

The adenine base of the nucleotide is bound in the back of the domain interface. The amino group (N6) forms a hydrogen bond to the backbone carbonyl of Glu147, and N1 accepts a proton from the backbone amide of Met149. Nonpolar interactions are found at both sides of the purine ring, including Ile70 and Val78 from the glycine-rich flap on one side, and Val196 from β7 on the other. The ribose O2′ and O3′ hydroxyls form a hydrogen-bonding network to the sidechain of Asn152 and the carbonyl group of Ser193. The triphosphate group forms many hydrogen bonds involving directly, or indirectly, most of the invariant amino acids of protein kinases. Hydrogen bonds to the phosphate oxygen atoms are formed by the mainchain

amide of Gln75 and the sidechains of Gln75 and Lys93. Comparison of different JNK isoform sequences shows that the amino acids involved in ATP binding are conserved [3].

Two magnesium ions (M1 and M2) are observed in the JNK3–MgAMP-PNP complex. The sidechain carbonyl group of Asn194 contacts metal ion M1, which in turn bridges the oxygens of the α- and γ-phosphoryl groups of AMP-PNP. Asp207 interacts through water molecules with M2, which is bound to the β- and γ-phosphoryl group oxygens. In contrast, the corresponding residue in cAPK (Asp184) coordinates both M1 and M2 directly. This significant difference may play a role in the low activity of the unphosphorylated conformation of the JNK3 enzyme. An important role in metal chelation has been proposed for Asp184 in cAPK, which requires direct interaction of the aspartic residue with the metal ion [16,20]. Asp207 is located within a loop called the 'DFG loop' which precedes the disordered β9 strand in unphosphorylated JNK3. The structure of JNK3 suggests that upon phosphorylation, the refolding of the phosphorylation lip and domain rotation should bring Asp207 closer to the nucleotide to allow its direct interaction with the metal ion.

Structural comparison of JNK3 and cAPK reveals that the two domains of JNK3 are rotated apart relative to their orientation in the structure of cAPK (Figure 3). This twist results in the misalignment of the two halves of the catalytic site of JNK3. In the N-terminal domain of JNK3, the putative catalytic residue Lys93 takes a position similar to its corresponding residue in cAPK and forms hydrogen bonds to the oxygen atoms of the α- and β-phosphoryl groups of the nucleotide. The catalytic loop (Arg188–Asn194) and the DFG loop (Asp207–Gly209) in the C-terminal domain are misaligned, however (Figure 4b). The conserved Asp189 and Asp207 residues are thought to be essential for protein kinase activity [21]. These residues are located 3 Å further away from Lys93 in JNK3, compared to their corresponding residues in cAPK. These differences suggest that the open conformation of the domains in JNK3 may contribute to the low activity of the unphosphorylated form of the enzyme.

The substrate specificity of JNK isoforms

The JNK3 binary complex is the first high-resolution structure to be determined within the JNK subfamily. In the region spanning residues Ser40–Ala418, JNK3 shares 92% and 87% amino acid identity with JNK1 and JNK2, respectively. Thus, the JNK3 structure provides a framework for understanding the substrate specificity of the different JNK isoforms. The nonconserved residues among JNK isoforms are clustered mainly in two regions (see Figure 1). One of these regions comprises the C-terminal portion of αF and the following loop L13. Most of the nonconserved residues in this region are solvent exposed and located on the protein surface corresponding to the

Figure 5
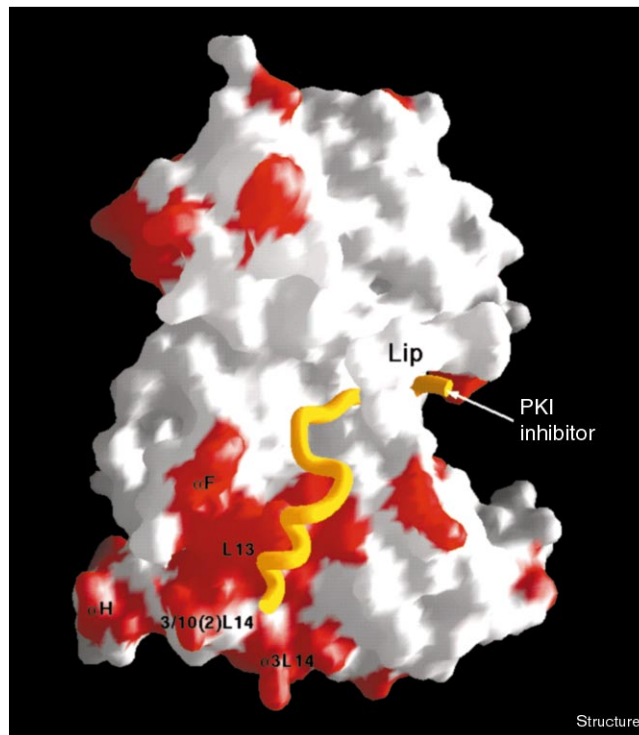
The substrate-binding specificity of JNK isoforms. The solvent-accessible surface of JNK3 is shown with the modeled PKI inhibitor (drawn as an orange tube) after the same superposition of the JNK3 and cAPK structures as described in Figure 3. Surface areas corresponding to the JNK3 residues not conserved in JNK1 and JNK2 are colored red. Two clusters of divergent regions of JNK isoforms, identified from the amino acid sequence alignment, are located next to each other on the protein surface in the C-terminal lobe. This area, containing αF and L13, has been shown to direct the substrate-binding specificity toward c-Jun [3]. (The figure was generated using the program GRASP [41].)

peptide substrate binding channel identified in cAPK (Figure 5). The position of these residues suggests that they have a role in substrate-binding specificity. In support of this hypothesis, the study of JNK chimeras has shown that JNK specificity towards c-Jun is directed to this region [22]. Furthermore, binding studies of JNK isoforms and various substrates have shown that JNK isoforms with higher homology in this region display similar binding selectivity towards similar substrates [3]. The other nonconserved region comprises α3L14 and the JNK insertion, which lies on the protein surface adjacent to the first nonconserved region (Figure 5). The location of this region suggests that it might be an extended substrate-binding site in JNK, and the sequence may be important for substrate-binding specificity.

Biological implications

The c-Jun N-terminal kinases (JNKs) are members of the mitogen-activated protein kinase family. JNKs are

serine/threonine kinases that are activated by dual phosphorylation of threonine and tyrosine residues. The phosphorylated residues (Thr221 and Tyr223) are located in a Thr-Pro-Tyr segment within the activation loop which is adjacent to the active site. A neuronal-specific isoform of JNK, JNK3, has been linked to neuronal apoptosis induced by kainic acid, indicating a role of JNK3 in the pathogenesis of glutamate neurotoxicity [12].

We report here the X-ray crystal structure of the unphosphorylated form of JNK3 in complex with MgAMP-PNP. The overall fold of JNK3 reveals similarities to the structures of cAMP-dependent protein kinase and two other MAP kinases, ERK2 and p38. Unphosphorylated JNK3 assumes an open conformation, in which the N- and C-terminal domains are oriented so that some of the catalytic residues are misaligned. In addition, the phosphorylated region of the protein, termed the 'phosphorylation lip' partially blocks the peptide substrate binding site. These structural features suggests that both global (domain closure to bring the catalytic residues in close proximity) and local (refolding of the lip to relieve steric constraints to substrate binding) conformational changes are required for JNK3 activation.

Crystallographic studies of ERK2, p38 and JNK3 have shown that the region spanning β strand β9 and the phosphorylation lip has the most diverse and labile conformation in unphosphorylated MAP kinases [13,14,23]. In the structure of phosphorylated ERK2, the conformation of this mobile region is stabilized by interactions formed between the phosphates and residues near the activation loop [19]. On the basis of the homology between ERK2 and JNK3, we propose that the phosphorylation of Thr221 and Tyr223 may have similar roles in activating JNK3 as they do in ERK2. In JNK3, phosphorylation of Thr221 could promote domain closure by interacting with Arg107 and Arg188, whereas phosphorylation of Tyr223 might result in new interactions with Arg227 and Arg230, which constitute part of the substrate-binding pocket.

Elevated activity of JNKs has been implicated in a variety of physiological processes ranging from T lymphocyte activation and apoptosis, to cardiac myocyte hypertrophy [24–27]. Modulation of JNKs could therefore provide therapeutic intervention for disorders such as autoimmune diseases, stroke, epilepsy and congestive heart failure. The structure reported here provides a framework for the design of selective JNK3 inhibitors.

Materials and methods
Expression and purification of JNK3
A search of the expression sequence tag (EST) database using the program BLAST and the published JNK3α1 cDNA [3] as a query identified an EST clone (#632588) that contained the entire coding sequence for human JNK3α1. Polymerase chain reactions (PCRs) using *Pfu* polymerase (Stratagene) were used to introduce restriction sites into the cDNA for cloning into the pET-15B expression vector at the *Nco*I and *Bam*HI sites; the construct was expressed in *Escherichia coli*. Due to the poor solubility of the expressed full-length protein (Met1–Gln422), an N-terminally truncated protein starting at Ser40 (corresponding to Ser2 of the JNK1 and JNK2 proteins [3]), preceded by methionine (initiation) and glycine residues, was produced. The glycine residue was added in order to introduce an *Nco*I site for cloning into the expression vector. Further, systematic C-terminal truncations were performed by PCR to identify a construct that gave rise to diffraction-quality crystals. The construct was prepared by PCR using two deoxyoligonucleotide primers – 5′ GCTCTAGAGCTCC*ATG*GGGCAGCAAAAGCAAAGTTG-ACAA 3′ (forward primer with initiation codon italicized) and 5′ TAGCG-GATCC*TCA*TTCTGAATTCATTACTTCCTTGTA 3′ (reverse primer with stop codon italicized) – and confirmed by DNA sequencing. The construct, which encodes amino acid residues Ser40–Glu402 of JNK3α1 preceded by methionine and glycine residues, was used for the structural studies described in this paper. Control experiments indicated that the truncated JNK3 protein has an equivalent kinase activity towards myelin basic protein when activated with an upstream kinase MKK7 [15] *in vitro* (TF and JTC, unpublished results).

E. coli strain BL21 (DE3) (Novagen) transformed with the JNK3 expression construct was grown at 30°C in shaker flasks into log phase (OD$_{600}$ ~ 0.8) in Luria broth supplemented with 100 μg/ml carbenicillin. Isopropyl-β-D-thiogalactopyranoside (IPTG) was then added to a final concentration of 0.8 mM and the cells were harvested 2 h later by centrifugation.

E. coli cell paste containing the truncated JNK3 protein was resuspended in 10 volumes/g lysis buffer (50 mM HEPES, pH 7.2, 10% glycerol [v/v], 100 mM NaCl, 2 mM dithiothreitol [DTT], 0.1 mM phenylmethylsulfonyl fluoride (PMSF), 2 μg/ml pepstatin, 1 μg/ml each of E-64 and leupeptin). Cells were lysed on ice using a microfluidizer and centrifuged at 100,000 × g for 30 min at 4°C. The 100,000 × g supernatant was diluted fivefold with buffer A (20 mM HEPES, pH 7.0, 10% glycerol [v/v], 2 mM DTT) and applied to an SP-Sepharose (Pharmacia) cation-exchange column at 4°C. The column was washed with five column volumes of buffer A, followed by five column volumes of buffer A containing 50 mM NaCl. Bound protein was eluted with a seven and a half column volume linear gradient of 50–300 mM NaCl and the truncated JNK3 protein was eluted between 150–200 mM NaCl. Eluted JNK3 protein from the SP–Sepharose column was dialyzed at ~ 1 mg/ml against buffer B (25 mM HEPES, pH 7.0, 5% glycerol [v/v], 50 mM NaCl, 10 mM DTT) overnight at 4°C and centrifuged at 3,000 × g. The supernatant was concentrated by ultrafiltration (Centriprep-30, Amicon) to 10 mg/ml, centrifuged at 16,000 × g and stored at −70°C.

Kinase assays
A coupled spectrophotometric assay was used in which ADP generated by activated JNK3 was converted back to ATP by pyruvate kinase (PK) with the concomitant production of pyruvate from phosphoenol pyruvate (PEP). Lactate dehydrogenase (LDH) reduces pyruvate to lactate with the oxidation of NADH. NADH depletion was monitored at 340 nm using a microplate reader for 20 min at 30°C. PK (100 μg/ml), LDH (50 μg/ml), PEP (2 mM) and NADH (200 μM) were added in large excess to the reaction buffer containing 50 mM HEPES, pH 7.6 and 10 mM MgCl$_2$. JNK3 activity was measured in the presence of 200 μM of an epidermal growth factor receptor peptide substrate (KRELVEPLTPSGEAPN-QALLR) and increasing concentration of ATP (2.5–800 μM) [28]. Reactions were initiated by the addition of 30 nM JNK3. Enzyme kinetic data were analyzed by nonlinear regression in the program EZ-Fit (Perrella Scientific, Amherst, NH). The specific kinase activities (k_{cat}/K_m) were 160,000 M^{-1}s^{-1} and 190,000 M^{-1}s^{-1} for the JNK3 lacking the N-terminal 39 residues (Ser40–Gln422) and the truncated JNK3 (Ser40–Glu402) used for crystallographic studies, respectively.

Crystallization
Crystallization trials were performed by combining the hanging-drop vapor diffusion technique and a sparse matrix search, in the presence

Table 1

Summary of data collection and structure refinement.

Data statistics	
Resolution (Å)	50–2.3
No. of reflections (measured/unique)	66 063/16 394
Completeness (overall/outer shell) (%)	90.0/75.4
R_{merge} (overall/outer shell) (%)*	5.2/16.5
Structure refinement†	
Resolution (Å)	30–2.3
No. of reflections	14 511
R factor	0.221
Free R factor‡	0.274
No. of water molecules	183
No. of AMP-PNP molecules	1
No. of Mg^{2+} ions	2
Rms deviations	
bonds lengths (Å)	0.009
bond angles (°)	1.5

*$R_{merge} = 100 \times \Sigma_h \Sigma_i \mid I_{hi} - <I_h> \mid / \Sigma_h \Sigma_i \mid I_{hi}$. †Values are given for data with $F > 2.0\sigma F$. ‡The free R factor [29] was calculated with 10% of the data.

and absence of MgAMP-PNP. No crystals were obtained in the absence of MgAMP-PNP, although crystallization trials carried out in the presence of MgAMP-PNP yielded an orthorhombic crystal form at 20°C over a reservoir solution containing 18–20% (v/v) polyethylene glycol monomethyl ether (average M_r = 550), 10% (v/v) ethylene glycol, 20 mM β-mercaptoethanol and 100 mM HEPES (pH 7.5). The crystallization droplet contained a mixture of 1 µl of reservoir solution plus 1 µl of a protein solution that had been preincubated for 1 h with 1 mM AMP–PNP and 2 mM $MgCl_2$ on ice. The crystals belong to the orthorhombic space group $P2_12_12_1$ (a = 51.50 Å, b = 71.24 Å and c = 107.60 Å) with one enzyme molecule per asymmetric unit. The solvent content of the crystal is 44%. Before data collection, crystals were equilibrated in their reservoir solution for 2–5 min before being flash-frozen in nitrogen gas for X-ray data collection at –170°C.

Data collection and structure determination
X-ray data were measured on an Raxis IIC image plate, with mirror-focused CuKα X-rays generated by a rotating-anode source. The diffraction images were processed with the program DENZO and data scaled using SCALPACK [29]. The data processing statistics are summarized in Table 1.

The starting phases for JNK3 were obtained by molecular replacement using coordinates of phosphorylated ERK2 (XX and KPW, unpublished results) as search model in the program AMoRe [30]. The ERK2 atomic model was modified by truncating to alanine for those residues that are different from JNK3 and deleting those loops that have significant insertions or deletions between ERK2 and JNK3. This hybrid model successfully produced rotation and translation function solution for JNK3, which provided a starting model with an R factor = 50% for reflections between 10 and 4.0 Å resolution at the start of the refinement. Refinement of the model using both conventional least-squares and simulated-annealing procedures was done with X-PLOR software [31] using 8–2.3 Å data. The electron density corresponding to the AMP-PNP molecule was visible from the map calculated using the initial model phases, but AMP-PNP was not included in the model refinement until the R factor dropped to 28% and the R free to 39%. The refined model, at 2.3 Å resolution (Table 1), includes 339 residues of JNK3, one AMP-PNP molecule, two Mg^{2+} and 183 water molecules. The electron-density maps revealed several discrete regions of disorder, leading to the omission of some amino acid residues from the final model. The N-terminal residues 40–44 and C-terminal residues 401 and 402 are disordered. In addition, two central regions of the enzyme are disordered,

including residues 212–216 and 374–378. Finally, the sidechain atoms for Tyr223 were not modeled beyond Cβ due to poor electron density. The present R factor is 22.4% (R free = 27.4%). Anisotropic scaling and bulk-solvent correction were applied at the final stage of the refinement [32]. The peptide torsion angles for 337 out of 339 well-defined residues fall within most favored or generally allowed regions of the Ramachandran plot, as defined in the program PROCHECK [33].

Accession numbers
The coordinates of the JNK3 structure have been deposited in the Protein Data Bank with accession code 1JNK.

References
1. Cobb, M.H. & Goldsmith, E.J. (1995). How MAP kinases are regulated. *J. Biol. Chem.* **270**, 14843-14846.
2. Minden, A. & Karin, M. (1997). Regulation & function of the JNK subgroup of MAP kinases. *Biochem. Biophys. Acta* **1333**, F85-F104.
3. Gupta, S., *et al.*, & Davis, R.J. (1996). Selective interaction of JNK protein kinase isoforms with transcription factors. *EMBO J.* **15**, 2760-2770.
4. Hibi, M., Lin, A., Smeal, T., Minden, A. & Karin, M. (1993). Identification of an oncoprotein and UV responsive protein kinase that binds and potentiates the c-Jun activation domain. *Genes Dev.* **7**, 2135-2148.
5. van Dam, H., Wilhelm, D., Herr, I., Stetfen, A., Herrlich, P. & Anglel, P. (1995). ATF-2 is preferentially activated by stress-activated protein kinases to mediate c-Jun induction in response to genotoxic agents. *EMBO J.* **14**, 1798-1811.
6. Whitmarsh, A.J., Shore P., Sharrocks, A.D. & Davis, R.J. (1995). Integration of MAP kinase signal transduction pathways at the serum response element. *Science* **269**, 403-407.
7. Chow, C.W., Rincon, M., Cavanagh, J., Dickens, M. & Davis, R.J. (1997). Nuclear accumulation of NFAT4 opposed by the JNK signal transduction pathway. *Science* **278**, 1638-1641.
8. Milne, D.M., Campbell, L.E., Campbell, D.G. & Meek, D.W. (1995). p53 is phosphorylated *in vitro* and *in vivo* by an ultraviolet radiation-induced protein kinase characteristic of the c-Jun kinase, JNK1. *J. Biol. Chem.* **270**, 5511-5518.
9. Zhang, Y., Zhou, L. & Miller, C.A. (1998). A splicing variant of a death domain protein that is regulated by a mitogen-activated kinase is a substrate for c-Jun N-terminal kinase in the human central nervous system. *Proc. Natl Acad. Sci. USA* **95**, 2586-2591.
10. Mohit, A.A., Martin, J.H. & Miller, C.A. (1995). p493F12 kinase: a novel MAP kinase expressed in a subset of neurons in the human nervous system. *Neuron* **14**, 67-78.
11. Martin, J.H., Mohit, A.A. & Miller, C.A. (1996). Developmental expression in the mouse nervous system of the p493F12 SAP kinase. *Brain Res. Mol. Brain Res.* **35**, 47-57.
12. Yang, D.D., *et al.*, & Flavell, R.A. (1997). Absence of excitotoxicity-induced apoptosis in the hippocampus of mice lacking the Jnk3 gene. *Nature* **389**, 865-870.
13. Zhang, F., Strand, A., Robbins, D., Cobb, M.H. & Goldsmith, E.J. (1994). Atomic structure of the MAP kinase ERK2 at 2.3 Å resolution. *Nature* **367**, 704-711.
14. Wilson, K.P., *et al.*, & Su, M.S.-S. (1996). Crystal structure of the P38 mitogen-activated protein kinases. *J. Biol. Chem.* **271**, 27696-27700.
15. Tournier, C., Whitmarsh, A.J., Cavanagh, J., Barrett, T. & Davis, R.J. (1997). Mitogen-activated protein kinase kinase 7 is an activator of the c-Jun NH_2-terminal kinase. *Proc. Natl Acad. Sci. USA* **94**, 7337-7342.
16. Bossemeyer, D., Engh, R.A., Kinzel, V., Ponstingl, H. & Huber, R. (1993). Phosphotransferase and substrate binding mechanism of the cAMP-dependent protein kinase catalytic subunit from porcine heart as deduced from a 2.0 Å structure of the complex with Mn^{2+} adenylyl imidodiphosphate and inhibitor PKI(5–24). *EMBO J.* **12**, 849-859.
17. Knighton, D.R., Zheng, J., Ten-Eyck, L.F., Xuong, N.-H., Taylor, S.S. & Sowadski, J.M. (1991). Structure of a peptide inhibitor bound to the catalytic subunit of cyclic adenosine monophosphate-dependent protein kinase. *Science* **253**, 414-420.

18. Zheng, J., *et al.*, & Sowadski, J.M. (1993). 2.2 Å refined crystal structure of the catalytic subunit of cAMP-dependent protein kinase complexed with MnATP and a peptide inhibitor. *Acta Cryst. D* **49**, 362-365.

19. Canagarajah, B.J., Khokhlatchev, A., Cobb, M.H. & Goldsmith, E.J. (1997). Activation mechanism of the MAP kinase ERK2 by dual phosphorylation. *Cell* **90**, 859-869.

20. Knighton, D.R., *et al.*, & Sowadski, J.M. (1991). Crystal structure of the catalytic subunit of cyclic adenosine monophosphate-dependent protein kinase. *Science* **253**, 407-413.

21. Gibbs, C.S., Knighton, D.R., Sowadski, J.M., Taylor, S.S. & Zoller, M.J. (1992). Systematic mutational analysis of cAMP-dependent protein kinase identifies unregulated catalytic subunits and defines regions important for the recognition of the regulatory subunit. *J. Biol. Chem.* **267**, 4806-4810.

22. Kallunki, T., *et al.*, & Karin, M. (1994). JNK2 contains a specificity-determining region responsible for efficient c-Jun binding and phosphorylation. *Genes Dev.* **8**, 2996-3007.

23. Zhang, J., Zhang, F., Ebert, D., Cobb, M.H. & Goldsmith, E.J. (1995). Activity of the MAP kinase ERK2 is controlled by a flexible surface loop. *Structure* **3**, 299-307.

24. Rincon, M. & Flavell, R.A. (1997). Regulation of the activity of the transcription factors AP-1 and NFAT during differentiation of precursor CD4$^+$ T-cells into effector cells. *Biochem. Soc. Trans.* **25**, 347-354.

25. Rincon, M. & Flavell, R.A. (1996). Regulation of AP-1 and NFAT transcription factors during thymic selection of T cells. *Mol. Cell. Biol.* **16**, 1074-1084.

26. Xia, Z., Dickens, M., Raingeaud, J., Davis, R.J. & Greenberg, M.E. (1995). Opposing effects of ERK and JNK-p38 MAP kinases on apoptosis. *Science* **270**, 1326-1331.

27. Wang, Y., Su, B., Sah, V.P., Brown, J.H., Han, J. & Chien, K.R. (1998). Cardiac hypertrophy induced by mitogen-activated protein kinase kinase 7, a specific activator for c-Jun NH$_2$-terminal kinase in ventricular muscle cells. *J. Biol. Chem.* **273**, 5423-5426.

28. Gonzalez, F.A., Raden, D.L. & Davis, R.J. (1991). Identification of substrate recognition determinants for human ERK1 and ERK2 protein kinases. *J. Biol. Chem.* **266**, 22159-22163.

29. Otwinowski, Z. (1993). Oscillation data reduction program. In *Data Collection and Processing, Proceedings of the National Study Weekend.* (Sawyer, L., Issacs, N. & Bailey, S.W., eds), pp. 55-62, Daresbury Laboratory, Warrington, UK.

30. Navaza, J. (1994). AmoRe: an automated package for molecular replacement. *Acta Cryst. A* **50**, 157-163.

31. Brünger, A.T. (1992). *X-PLOR*, *Version 3.1 Manual.* Yale University Press, New Haven, CT.

32. Brünger, A.T., *et al.*, & Warren, G.L. (1998). Crystallography and NMR system: a new software system for macromolecular structure determination. *Acta Cryst. D*, in press.

33. Laskowski, R.A., MacArthur, M.W., Moss, D.S. & Thornton, J.M. (1993). Procheck: a program to check the stereochemical quality of protein structures. *J. Appl. Cryst.* **26**, 283-291.

34. Lee, J.C., *et al.*, & Young, P.R. (1994). A protein kinase involved in the regulation of inflammatory cytokine biosynthesis. *Nature* **372**, 739-746.

35. Boulton, T.G., *et al.*, & Yancopoulos, G.D. (1991). ERKs: a family of protein-serine/threonine kinases that are activated and tyrosine phosphorylated in response to insulin and NGF. *Cell* **65**, 663-675.

36. Uhler, M.D. (1986). Isolation of cDNA clones coding for the catalytic subunit of mouse cAMP-dependent protein kinase. *Proc. Natl Acad. Sci. USA* **83**, 1300-1304.

37. Hanks S.K., Quinn, A.M. & Hunter, T. (1988). The protein kinase family: conserved features and deduced phylogeny of the catalytic domains. *Science* **241**, 42-52.

38. Derijard, B., *et al.*, & Davis, R.J. (1994). JNK1: a protein kinase stimulated by UV light and Ha-Ras that binds and phosphorylates the c-Jun activation domain. *Cell* **76**, 1025-1037.

39. Sluss, H.K., Barrett, T., Derijard, B. & Davis, R.J. (1994). Signal transduction by tumor necrosis factor mediated by JNK protein kinase. *Mol. Cell. Biol.* **14**, 8376-8384.

40. Carson, M. (1991). Ribbons 2.0. *J. Appl. Cryst.* **24**, 958-961.

41. Nicolls, A., Sharp, K.A. & Honig, B. (1991). Protein folding and association: insights from the interfacial and thermodynamic properties of hydrocarbons. *Proteins* **11**, 281-296.